X-Ray Astronomy 2000
ASP Conference Series, Vol. 234, 2001
R. Giacconi, S. Serio and L. Stella, eds.

New insights on Radio-Galaxy X-ray Emission Components from *Chandra*

D.M. Worrall, M. Birkinshaw & M.J. Hardcastle

Department of Physics, University of Bristol, Tyndall Avenue, Bristol BS8 1TL, UK

Abstract.
The superior spatial resolution of the *Chandra X-ray Observatory* is sharpening our X-ray view of extragalactic radio sources. We have discovered new X-ray hotspots or jets in most of our early *Chandra* observations. We discuss several well-known sources (such as 3C 123, PKS 0521-365, and 3C 220.1) and a subset of the complete B2 radio-galaxy sample. We conclude that X-ray jets are common in low-power radio galaxies and are more readily detected in ~ 7 ks exposures with *Chandra* than in the optical via HST snapshot surveys. We describe some early implications of the results for the energetics and dynamics of extragalactic jets.

1. Introduction

X-ray observations made before *Chandra* showed that radio galaxies are complex X-ray emitters, and there are examples where the emission arises from hot gas held in the potential well of the group/cluster, from inverse Compton or synchrotron processes in radio lobes, hotspots and jets, and from the active-galaxy cores (see Worrall 2000 for a review). In a few cases, notably Cygnus A, there is a component of heavily absorbed X-ray emission from the core, thought to originate close to the AGN. However, most sources have soft compact X-ray emission. The radio to soft X-ray two-point spectral index, $\alpha_{\rm rx}$, is ~ 0.85 for cores of low-power radio galaxies. High-power sources show a similar $\alpha_{\rm rx}$ where the radiation is undoubtedly radio related and highly beamed (core-dominated quasars) or where any contribution from the inner AGN-related regions is thought to suffer high absorption (narrow-line radio galaxies), but in broad emission-line objects, such as lobe-dominated quasars, a flatter $\alpha_{\rm rx}$ is normally seen, and this is believed to be due to regions close to the AGN dominating the central X-ray output. A value of $\alpha_{\rm rx} \sim 0.85$ is also measured in resolved knots in the jets of the nearby radio galaxies Cen A and M 87, and this has led us to suggest that radio-related X-ray emission with this $\alpha_{\rm rx}$ is generally present at parsec to perhaps kiloparsec distances from the cores (Worrall 1997).
The pre-*Chandra* imaging observations of highest spatial resolution were made with ROSAT. It is only in the nearest and brightest sources that it is possible to say with confidence that small-scale non-thermal emission has been detected, since ROSAT's spatial resolution and sensitivity were insufficient to distinguish between truly small-scale nonthermal emission and small-scale hot gas, possi-

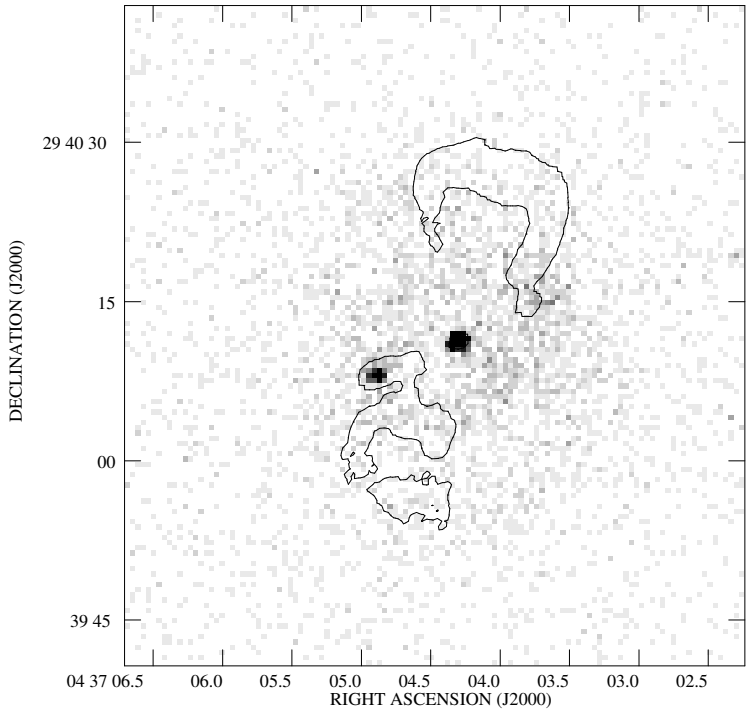

Figure 1. The 3 mJy/beam contour from an 8.4 GHz VLA radio map is overlayed on the 38.5 ks-exposure *Chandra* ACIS image of the $z = 0.2$ powerful radio galaxy 3C 123. In addition to extended X-ray emission from cluster gas, X-ray emission from the core and eastern hotspot complex are clearly visible. (From Hardcastle et al. 2001)

bly associated with cooling flows. Furthermore, most ROSAT observations were made with the HRI and yielded no spectral information. The arcsec spatial resolution of *Chandra* now puts radio galaxies in sharp focus, with spatial resolution in a typical low-power radio galaxy at $z = 0.035$ of ~ 1 kpc, and a high-power radio galaxy at $z = 0.6$ of ~ 9 kpc (for $H_o = 50$ km s^{-1} Mpc^{-1}, $q_o = 0$). Here we discuss examples of both high- and low-power sources observed as part of our AO1 Guest Observer programs with the ACIS instrument.

2. Testing equipartition with X-ray observations

In simple terms, radio synchrotron luminosity (L_s) depends on three parameters: relativistic electron density (n_e), volume (V), and magnetic field strength (B). In radio hotspots, V and L_s are well measured, leaving one equation and two unknowns. It is usual to assume that B takes on the equipartition value, $B_{\rm eq}$, for which the electron and magnetic-field energy densities are equal (roughly equivalent to the minimum energy condition). With this extra constraint, n_e and $B = B_{\rm eq}$ can be found from the radio data alone.

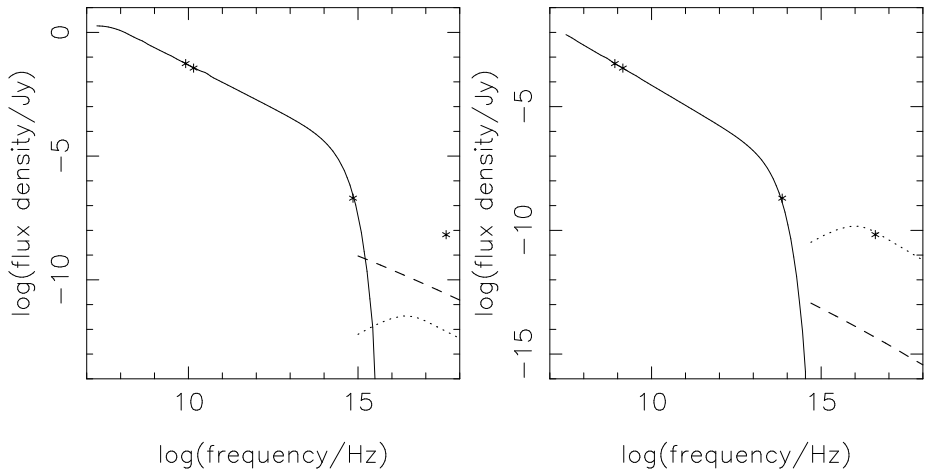

Figure 2. Rest-frame spectral energy distributions of the WK7.8 knot in the jet of PKS 0637-752 (Chartas et al. 2000; Schwartz et al. 2000). Model fits show synchrotron emission as solid line, SSC as dashed, and up-scattering of the CMB as dotted. Left: model assumes $B = B_{\rm eq}$ with negligible relativistic beaming in the jet. SSC fails to predict the X-ray under this assumption for B. Right: model assumes $B = B_{\rm eq}$, and a jet with $\beta = 0.9987$ at 5° to the line of sight.

X-ray measurements are uniquely able to test the assumption that $B = B_{\rm eq}$ in the situation where the X-rays arise from up-scattering of a well-determined photon field, such as in the well-known synchrotron self-Compton (SSC) process where the scattered photons are the radio synchrotron emission. The measured X-ray luminosity ($L_{\rm ic}$) then depends on n_e, V, and synchrotron photon density, and the two equations with two unknowns allow B and n_e to be determined.

For 3C 123 we predicted that with SSC and $B = B_{\rm eq}$, X-rays should be detected from the eastern, but not western, hotspot complex in a $\sim$ 40 ks ACIS observation. Results (Fig. 1) strikingly confirm the prediction. While there are some caveats, since other contributions to the hotspot-X-rays are possible, the closeness of the prediction to the measured level of X-rays argues in favor of a dominance of the SSC process, and we find a best fit of $B \sim 0.7 B_{\rm eq}$ (Hardcastle et al. 2001). Earlier measurements with ROSAT for Cygnus A (Harris et al. 1994) and with *Chandra* for 3C 295 (Harris et al. 2000) came to a similar conclusion, that the magnetic fields in hotspots are close to their equipartition values.

Reasons hotpots are good sites for testing equipartition are that the volume is well known and relativistic beaming and projection effects are not believed to be important. With sufficient X-ray spatial resolution, tests can extend to jets, as dramatically shown by ACIS's first science target, the $z = 0.65$ radio-loud quasar PKS 0637-752, which revealed a large resolved X-ray jet for which an SSC interpretation finds a value of B very far from $B_{\rm eq}$ (Chartas et al. 2000; Schwartz et al. 2000; Fig. 2 left), using the constraint placed on the electron spectrum by the level of optical jet emission detected with HST. A way to recover an equipartition magnetic field (Tavecchio et al. 2000) is to assume that the highly

relativistic jet ($\beta \sim 0.9987$) seen at small angles to the line of sight in VLBI data does not measurably decelerate out to a distance of ~ 1 Mpc, in which case the X-rays can arise from up-scattering of the boosted (in the jet frame) cosmic-microwave-background (CMB) radiation field (Fig. 2 right). Such a large fast jet may then make PKS 0637-752 an extreme object, since statistical studies of the structures of radio sources suggests that jet velocities average only about $0.7c$ at distances of tens of kpc from the core (Wardle & Aaron 1997; Hardcastle et al. 1999). Table 1 lists values of $\alpha_{\rm rx}$ for the core and jet of PKS 0637-752, based on measurements in Chartas et al. (2000), together with some other sources discussed in this paper.
Chandra observations of slow jets, such as the kpc-scale jets of low-power radio sources (Laing et al. 1999), reduce one uncertainty in deciding if equipartition magnetic fields hold. Here the predicted level of up-scattered CMB radiation (unboosted in the jet frame) is small. The nearby radio galaxy NGC 4261 is one such example where we detect X-ray jet emission and where HST measurements constrain the electron spectrum in such a way that an SSC model requires B far from $B_{\rm eq}$ (Birkinshaw et al., in preparation).

3. X-ray jets in low-power radio galaxies

Our first observations with *Chandra* of low-power radio galaxies have been short ($\sim$ 7 ks) ACIS exposures of B2 0206+35, 0331+39, and 0755+37 (Worrall et al. 2001a). In B2 0206+35 (Figs. 3,4) and 0755+37 we see three X-ray components within the scale of the optical galaxy: (i) emission associated with the prominent radio jets of $2''$ and $4''$ length, respectively, (ii) an unresolved component coincident with the radio nucleus, and (iii) emission from galaxy-scale gas of central pressure similar to the minimum pressure in these radio jets, and which may therefore play a role in the jet dynamics. In B2 0331+39 there is no obvious radio jet, either because of small viewing angle, which could superimpose the jet X-ray emission on the core, or because well-collimated kpc-scale plasma is simply absent in this source. The X-ray emission is unresolved.

Chandra resolves some of the emission we had previously associated with the cores, based on ROSAT (Canosa et al. 1999), and our revised measurements of $\alpha_{\rm rx}$ for the cores have increased somewhat (Table 1). Since the core X-ray emission is not heavily absorbed and has an $\alpha_{\rm rx}$ similar to that in the two jets, it most plausibly arises from sub-kpc-scale radio structures, a smaller-scale version of the kpc-scale jet-related emission seen in B2 0206+35 and 0755+37. While we detect X-ray jets in two out of our three sample sources, and both of those with kpc-scale radio jets, Capetti et al. (2000) report detection of only three of 57 representative B2 radio galaxies observed in an HST snapshot survey, even though roughly 45% of all B2 radio galaxies have kpc-scale radio jets (Parma et al. 1987). kpc-scale radio jets are detected in the X-ray in $\sim$ 7 ks exposures with *Chandra* more readily than in the optical via HST snapshot surveys.
To test the contending emission mechanisms of synchrotron radiation or inverse Compton scattering requires the deeper observations and larger samples of our ongoing work. We are currently analyzing data for two other B2 radio galaxies observed more recently with *Chandra*, and both show jet features. BL Lac

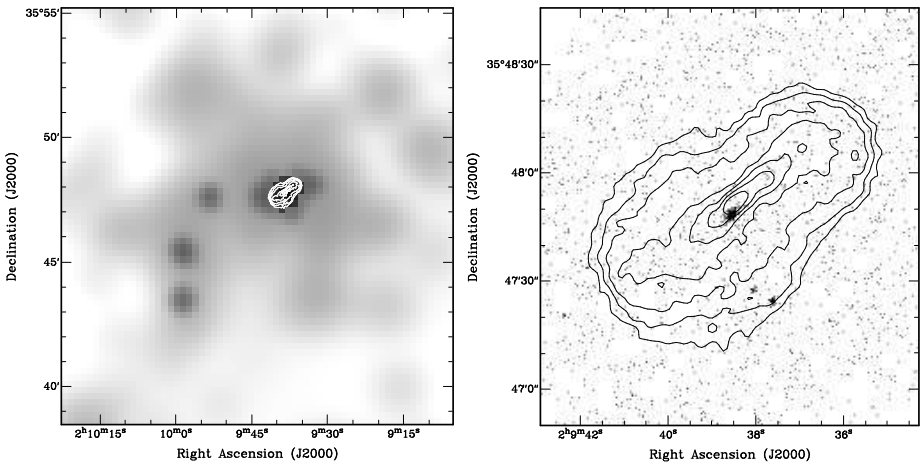

Figure 3. Low-resolution (1.4 GHz) radio contours of B2 0206+35 on image from the ROSAT PSPC (left; Worrall & Birkinshaw 2000), preferentially detecting cluster gas, and *Chandra* (right).

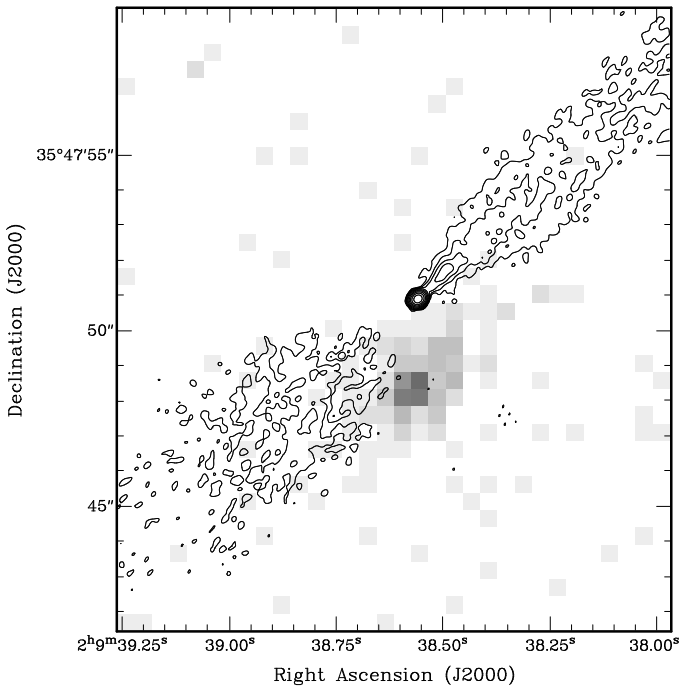

Figure 4. Magnified view of B2 0206 with high-resolution (8.4 GHz) contours on the *Chandra* image shows X-ray extension along the radio jet; the offset between the cores is a known problem with the astrometry applied to these *Chandra* data, uncorrected here for clarity. The *Chandra* data fit emission from core + jet and galaxy-scale gas (Worrall et al. 2001a).

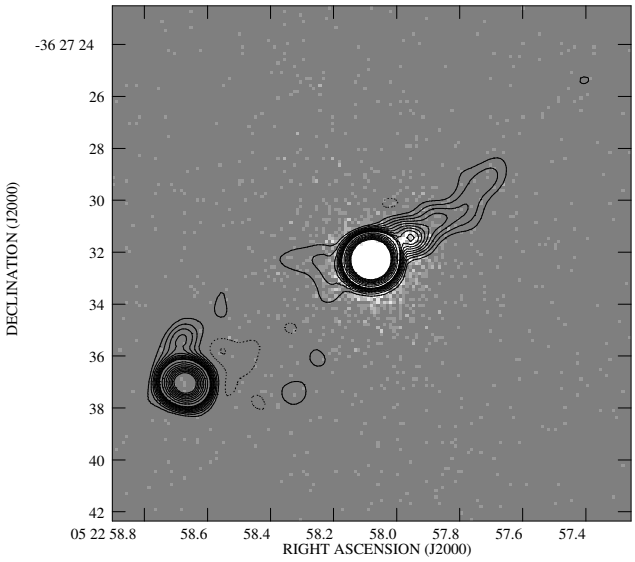

Figure 5. Contours from an 8.6 GHz ATCA radio map are overlayed on the 10 ks-exposure *Chandra* image of the $z = 0.055$ BL Lac object PKS 0521-365. The radio core (whose contours are suppressed) is bright in X-rays. *Chandra* detects X-ray emission from the NW radio jet. (From Birkinshaw et al. 2001)

objects are believed to be low-power radio galaxies whose jets are at a small angle to the line of sight, and despite the resulting foreshortening of the jet, *Chandra* has detected jet X-rays in PKS 0521-365 (Fig. 5). At the spatial resolution possible with *Chandra*, X-ray jets are indeed common.

4. High-power Radio Galaxy 3C 220.1

Figure 6 shows results from our 18 ks exposure with ACIS of the high-power radio galaxy 3C 220.1, at $z = 0.62$ (Worrall et al. 2001b). Our modeling of the ROSAT HRI data for the source as a composite of point-like and extended emission (Hardcastle et al. 1998) is strikingly confirmed by the new data.
The cluster should be in a giant cooling flow, since the cooling time is shorter than the Hubble time out to a radius of about $15''$, but the core X-ray emission is too spiked towards the center for a straightforward model including a large cooling flow. Indeed, the central data fit the PRF well. If we associate the central X-ray emission within the PRF with the radio core, its $\alpha_{\rm rx}$ (Table 1) is less than for other sources, suggesting perhaps that regions close to the AGN dominate the central X-ray output, as is believed to be the case for lobe-dominated quasars (see Section 1).

Acknowledgments. We thank Raffaella Morganti and Guy Pooley for providing 1.4 GHz data on B2 0206+35 and 8.4 GHz data on 3C 220.1, respectively, and John Biretta for use of his 8.4 GHz archival data on B2 0206+35. We thank staff of the Chandra X-ray Center for help with calibrations and software.

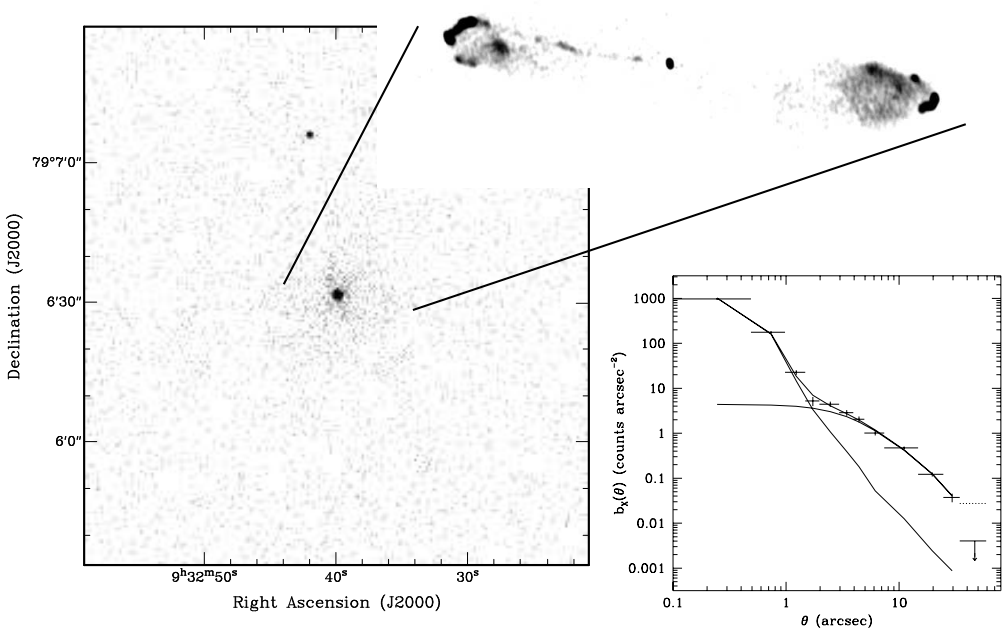

Figure 6. Main picture on left is the 18 ks-exposure *Chandra* image centered on the $z = 0.62$ radio galaxy 3C 220.1. An unrelated X-ray point source lies to the north. The insert shows an 8.4 GHz VLA radio image of 3C 220.1. On the right is the background-subtracted radial profile of the X-ray data for 3C 220.1 with the best-fit model of point-like emission plus a β-model ($\beta = 0.5$, core radius = 3.55 arcsec). The contribution of the model to the background region, taken into account in the fitting, is shown dotted. (From Worrall et al. 2001b)

Table 1. $\alpha_{\rm rx} = \log(l_{5\ {\rm GHz}}/l_{2\ {\rm keV}})/7.98$ for radio-source cores & jets

Source	z	type	core $\alpha_{\rm rx}$	jet $\alpha_{\rm rx}$
B2 0206+35	0.0369	low-power radio galaxy	0.91	0.88
B2 0331+39	0.0204	low-power radio galaxy	0.83	–
B2 0755+37	0.0428	low-power radio galaxy	0.85	0.88
3C 220.1	0.62	high-power radio galaxy	0.75	–
PKS 0637-752[a]	0.653	high-power quasar	0.92	0.90

a. core and jet (knot WK7.8) flux densities from Chartas et al. (2000)

References

Birkinshaw, M., Worrall, D.M. & Hardcastle, M.J. 2001, MNRAS, submitted

Canosa, C.M., Worrall, D.M., Hardcastle, M.J. & Birkinshaw, M. 1999, MNRAS, 310, 30

Capetti, A., de Ruiter, H.R., Fanti, R., Morganti, R., Parma, P. & Ulrich, M.-H. 2000, A&A, 362, 871

Chartas, G. et al. 2000, ApJ, 543, 655

Hardcastle, M.J., Lawrence, C.R. & Worrall, D.M. 1998, ApJ, 504, 743

Hardcastle, M.J., Alexander, P., Pooley, G.G. & Riley, J.M. 1999, MNRAS, 304, 135

Hardcastle, M.J., Birkinshaw, M. & Worrall, D.M. 2001, MNRAS, in press

Harris, D.E., Carilli, C.L. & Perley, R.A. 1994, Nature, 367, 713

Harris, D.E. et al. 2000, ApJ, 530, L81.

Laing, R.A., Parma, P., de Ruiter, H.R. & Fanti, R. 1999, MNRAS, 306, 513

Parma, P., Fanti, C., Fanti, R., Morganti, R. & de Ruiter, H.R. 1987, A&A, 181, 244

Schwartz, D.A. et al. 2000, ApJ, 540, L69

Tavecchio, F., Maraschi, L., Sambruna, R.M. & Urry, C.M. 2000, ApJ, 544, L23

Wardle, J.F.C. & Aaron, S.E. 1997, MNRAS, 286, 425

Worrall, D.M. 1997, in *Relativistic Jets in AGNs*, ed. M. Ostrowski et al. (Astronomical Observatory of the Jagiellonian University, Krakow), 20

Worrall, D.M. 2000, in *Life Cycles of Radio Galaxies*, ed. J Biretta et al., New Astronomy Reviews (Elsevier Science), astro-ph/9911056

Worrall, D.M. & Birkinshaw, M. 2000, ApJ, 530, 719

Worrall, D.M., Birkinshaw, M. & Hardcastle, M.J. 2001a, MNRAS, submitted

Worrall, D.M., Birkinshaw, M., Hardcastle, M.J. & Lawrence, C.R. 2001b, MNRAS, submitted